applied sciences

MDPI

Article

Comparison between Design Formulations and Numerical Results for In-Plane FRCM-Strengthened Masonry Walls

Giovanni Crisci [1], Francesca Ceroni [1,*] and Gian Piero Lignola [2]

[1] Department of Engineering, University of Naples "Parthenope", Centro Direzionale C4, 80143 Naples, Italy; giovanni.crisci@uniparthenope.it

[2] Department of Structures for Engineering and Architecture, University of Naples "Federico II", Via Claudio 21, 80125 Naples, Italy; glignola@unina.it

* Correspondence: francesca.ceroni@uniparthenope.it

Received: 16 June 2020; Accepted: 17 July 2020; Published: 21 July 2020

Abstract: Strengthening strategies and structural rehabilitation of existing buildings with innovative materials and techniques are today one of the main activities in the field of structural engineering. Externally bonded Fiber Reinforced Cementitious Matrix (FRCM), materials are spreading as an alternative strengthening technique to the more traditional Fiber Reinforced Polymer (FRP) ones, especially for masonry elements. This research focuses on the assessment of the shear strength of in-plane FRCM-strengthened masonry walls by means of code predictions and numerical results, with particular attention on the interpretation of diagonal compression tests simulated by means of Finite Element (FE) models. Firstly, the various approaches commonly adopted for the interpretation of diagonal compression tests in terms of shear strength were examined, since codes give generally provisions in terms of maximum shear force, while several experimental and numerical results of diagonal compression tests are available in literature. Then, the numerical simulations of diagonal compression tests obtained by several FE analyses in a previous work were examined in light of these different approaches; the corresponding predictions of the shear force are compared with code indications in order to individuate the most reliable approach both for the un-strengthened and the FRCM-strengthened walls. For the latter ones, a detailed analysis of the actual strain levels in the reinforcement was carried out, too, by means of FE analysis.

Keywords: FRCM; masonry; diagonal compression test; shear strength; Finite Element Model (FEM)

1. Introduction

Masonry constructions are a large part of the worldwide existing buildings, especially in Italian city centers; they represent an important historical and cultural heritage which needs to be preserved. The recent earthquakes, especially the last large ones that hit the Central Italy with several events in 2016–2017, confirmed the high seismic vulnerability of masonry constructions (Cescatti et al., 2020 [1]). This raised the interest of the scientific community to improve the masonry seismic capacity through the use of new techniques and innovative materials. In last decades, new strengthening and repair systems were developed and studied, based on the use of Fiber Reinforced Polymers (FRP) and Fiber Reinforced Cementitious Matrices (FRCM) materials. The first ones are based on the use of high strength fibers bonded by means of epoxy resins, mainly oriented in only one direction, on concrete, masonry, steel, or wooden substrates (Council of National Research (CNR) DT200/R1, 2013 [2]; CNR DT201, 2005 [3], CNR DT202, 2005 [4]). The use of epoxy for both impregnating and bonding the fibers allows realizing very thin strengthening systems, with no mass increase and stiffness. The FRCM materials are becoming

very diffuse in the last years, especially for strengthening of masonry elements, due both to the use of cement-based matrices, which are more compatible with the masonry substrates than the epoxy, and to the "grid" configuration of the fibers, which are usually oriented according to two orthogonal directions and are thus more suitable to adsorb multidirectional stress distributions in masonry walls. Moreover, such a technique is less sensitive to the debonding phenomena that affect the FRP materials (CNR DT200/R1, 2013 [2]), and, in comparison with the traditional use of reinforced concrete layers, it allows to reduce the thickness of the strengthening intervention to only 10–15 mm.

Due to the great interest in the application of FRCM systems, many experimental studies have been carried out by means of both tensile tests, aimed to characterize their mechanical behavior, and of bond tests, aimed to investigate the bond performance when applied on concrete or masonry substrates (D'Ambrisi et al., 2013 [5], Carozzi et al., 2016 [6], Bilotta et al., 2017a [7], Bilotta et al., 2017b [8], Ceroni and Salzano, 2018 [9]). Moreover, by means of experimental tests or analytical approaches, FRCM materials were analyzed as strengthening systems for several masonry elements subjected to in plane (Papanicolau et al., 2011 [10]) or out plane (Ramaglia et al., 2019a [11], Ramaglia et al., 2019b [12]) loading conditions. Within the numerical investigations, several studies available in literature are focused on the most suitable modeling strategies for simulating both the behavior in tension of FRCM systems and the global behavior of masonry walls strengthened with these materials (Bertolesi et al., 2014 [13], Bernardi et al., 2016 [14], Lignola et al., 2019 [15], Nerilli et al., 2020 [16]).

The experimental assessment of the shear strength of masonry walls was diffusely carried out by means of "diagonal-compression" tests (Brignola et al., 2008 [17], Calderini et al., 2009 [18], Magenes and Calvi, 1997 [19]). This kind of test is quite simple to realize in a laboratory and has been largely diffused to also estimate the effectiveness of innovative materials (Parisi et al., 2013 [20], Babaeidarabad et al., 2013 [21], Ferretti et al., 2016 [22], Del Zoppo et al., 2019 [23]). In such a test, a square masonry wall is loaded in compression, along one diagonal, up to failure, which is usually characterized by formation of cracks along the loaded diagonal, i.e., a "diagonal cracking shear" failure.

The shear strength can be evaluated with the shear-compression test, as well, but this type of set-up is more complicated to realize in a laboratory, especially if the compression load has to remain centered and no rotations are expected on the top side of the specimen during the tests, so that complex mechanical or electronic controlling systems have to be planned to these aims (Magenes et al., 2010 [24], Türkmen et al., 2019 [25]). Typically, large specimens are used in this test set-up in order to investigate the wall shape ratio too. The specimens are subjected to a fixed level of vertical compression and, then, a lateral force, pushing or pulling, static or dynamic, is applied at the top of masonry wall up to failure, which can be "flexural" or due to "sliding shear" or "diagonal cracking shear".

On the predictions of shear strength of masonry walls, literature and code indications generally give provisions in terms of maximum shear force, depending on the level of compression stress applied to the wall. Thus, the maximum force experimentally attained in shear-compression tests can be directly compared with theoretical provisions, while the maximum compression force obtained in diagonal-compression tests has to be firstly correlated to a shear force before comparing with code indications.

In addition, the recent Italian guidelines for design of strengthening interventions with FRCM materials (CNR DT 215, 2018 [26]) provide indications for calculating the in-plane contribution of the FRCM reinforcement in terms of shear force, which has to be added to the shear strength of the un-strengthened masonry wall.

Thus, starting from the numerical results of several FE analyses concerning diagonal-compression tests previously carried out by the authors by means of the DIANA TNO software, the paper is focused on:

1. evaluating the shear strength of the investigated masonry panels based on the maximum compression force achieved by the FE models both for the un-strengthened and the in-plane FRCM-strengthened walls according to different approaches suggested in literature;

2. comparing the shear strengths obtained by the numerical models with the theoretical values given by code formulations and assessing which approach is the most suitable to determine the shear capacity from the diagonal compression test.

It is worthy of note that the second point is based on the assumption that numerical results from validated models are equivalent to experimental ones, since several studies (Lourenco, 1996 [27], Grande et al., 2008 [28], Lignola et al., 2012 [29], Grande et al., 2013 [30], Parisi et al., 2013 [31], Ceroni et al., 2014 [32], Garofano et al., 2016 [33]) are already available in literature on the reliability of FE models, and most of them are specifically implemented in DIANA TNO software, to correctly predict the experimental outcomes. In particular, most studies concern the simulation of masonry walls subjected to a diagonal compression force, since this kind of test is simpler to realize, as previously commented. Numerical simulations allow for carrying out wide parametric analyses that would be very consuming in terms of time and money if carried out by means of experimental tests and allowing for investigation of the effect of parameters that can be hardly varied in experimental tests or that are uncertain to be evaluated. Conversely, the theoretical formulations available in literature or provided by codes depend on few parameters (mainly the tensile or the shear strength of masonry and the wall geometry), which are not able to completely catch the variability of the real behavior of masonry panels. Thus, the paper focuses on the agreement of these formulations when compared with the results of wide spectrum parametric numerical analysis.

2. Code Provisions for Shear Strength of In-Plane FRCM Strengthened Masonry Panels

According to the novel Italian guidelines for strengthening with FRCM materials (CNR DT 215 2018 [26]), the capacity of the strengthened walls with FRCM composite material can be evaluated as the sum of two contributions (Lignola et al., 2018 [34]): the shear strength of the un-strengthened walls, V_t, evaluated according to the current Italian code (IBC, 2018 [35], IBCC, 2019 [36]) for un-strengthened walls in case of "diagonal cracking" failure, plus the strength contribution of the composite, $V_{t,f}$, computed according to the following formulation:

$$V_{t,f} = \frac{n_f \cdot t_{Vf} \cdot \ell_f \cdot \alpha_t \cdot \varepsilon_{fd} \cdot E_f}{2}, \quad (1)$$

where 2 is a safety factor related to the calculation of a design value, n_f is the total number of reinforcement layers placed on the two sides of the wall, t_{Vf} is the equivalent thickness of a single reinforcement layer with fibers arranged along the direction parallel to the shear force, ℓ_f is the size of the strengthening system measured orthogonally to the shear force—and, in any cases, it cannot be greater than the width of the wall l (dimension measured parallel to the shear force)—, α_t is a parameter that takes into account the reduced exploitation of the fibers when stressed in shear (0.8 is the suggested value lacking experimental information), and ε_{fd} is the design value of the maximum strain of the fibers that can be assumed equal to a conventional strain evaluated as:

$$\varepsilon_{f,d} = \frac{\sigma_{\text{lim},conv}}{E_f} \quad (2)$$

with E_f being the Young's modulus of the dry fibers. The conventional tensile stress, $\sigma_{lim,conv}$, should be evaluated according to bond tests carried out on the FRCM system bonded on a specific masonry substrate and could be further increased by a factor α, variable in the range 1.0–1.5, if the failure mode does not involve an anchorage zone of the reinforcement. Moreover, the value of $\sigma_{lim,conv}$ cannot be higher than the tensile strength of the fibers, evaluated by means of tensile tests on FRCM coupons (de Felice et al., 2018 [37]).

It is worthy of note that, in several experimental programs concerning tests on masonry walls (De Santis et al., 2019 [38], D'Ambra et al., 2018 [39], D'Ambra et al., 2019 [40]), no bond tests are performed on the same strengthening material; this means that it is not possible to compare the

maximum tensile strain attained in the FRCM reinforcement when applied on the walls with the values provided by bond tests on the same type of reinforcement and masonry and thus assess the conventional strain or stress. Consequently, some uncertainness about the assessment of the conventional tensile strain or stress in the FRCM reinforcement does exist. To fill this gap, in Section 5.2, some considerations about the assessment of the strain levels in the FRCM reinforcement when the walls fail will be carried out.

On the behavior of un-strengthened masonry walls, the simplified models available in the scientific literature and in several national codes are intended to describe the different failure modes that can occur in masonry walls when subjected to in-plane horizontal forces, such as flexural or shear failures. With reference to shear failures, two main types of behavior can be detected in masonry walls: (1) shear failure for sliding along the mortar joints, typical of regular masonry and usually predicted by the Mohr-Coulomb criterion, and (2) diagonal cracking failure. The latter can occur according to further modalities: (2a) failure in the mortar joints, mainly typical of regular wall texture, and (2b) cracks intersecting the units, typical of irregular masonry texture. In particular, for the failure mode characterized by diagonal cracking, two approaches are available in literature and are recalled in the Italian code (IBC, 2018 [35]) and commentary (IBCC, 2019 [36]):

(a) models that describe the masonry as an equivalent isotropic material and consider the development of cracks along the main directions of tension, as the one proposed by (Turnšek and Čačovič, 1970 [41]); these approaches suppose the tensile failure occurs in the masonry units;

(b) models that describe the masonry as a composite material as the one proposed by (Mann and Müller, 1980 [42]) and suppose separately the development of cracks along its constituent components, i.e., mortar joints and blocks. In particular, when cracks occur in the mortar, the strength formulations depend on equivalent parameters of masonry, which are functions of local parameters (i.e., shear strength for sliding in absence of normal stress and friction coefficient) and of an interlocking masonry factor.

The approach proposed by (Turnšek and Čačovič, 1970 [41]) has the advantage of using a single mechanical parameter f_t, i.e., the masonry's tensile strength, completely neglecting the actual anisotropy of the masonry. The Italian code, starting from the one dated back 1996 (D.M. 09/01/1996 [43]), adopts such an approach to estimate the shear strength of masonry walls in case of diagonal cracking of masonry units for existing buildings made of irregular texture masonry or, according to a safe approach, allows to use it also for diagonal cracking in regular masonry walls:

$$V_t = l \cdot t \cdot \frac{f_{td}}{b} \cdot \sqrt{1 + \frac{\sigma_{od}}{f_{td}}}, \tag{3}$$

where l and t are the length and the thickness of the wall, respectively (see Figure 1a), σ_{0d} is the mean normal stress acting on the wall and referred to the gravitational load applied on the total area of the cross section ($l \cdot t$), and f_{td} is the design value of the tensile strength of masonry for diagonal cracking. Alternatively, the parameter f_{td} can be also expressed as $1.5 \cdot \tau_{od}$, with $\cdot \tau_{od}$ being the pure shear strength, in agreement with the original formulation of Reference [41]. In addition, the Italian code provides the parameter b, which is related to the stress distribution on the section and depends on the slenderness of the masonry wall: it can be assumed as $b = h/l$, and, in any case, it must not be greater than 1.5 and not smaller than 1, with h being the height of the wall.

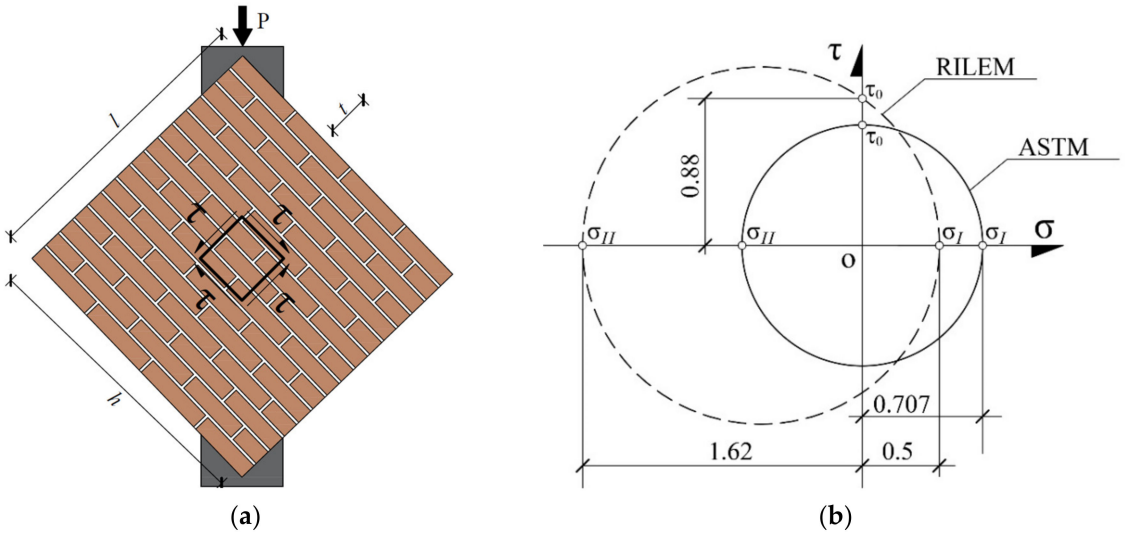

Figure 1. (**a**) American standard (ASTM) interpretation of the diagonal compression test; (**b**) Mohr's circle corresponding to ASTM and RILEM interpretation of diagonal compression test.

As previously explained, the Italian guidelines for design with FRCM materials (CNR DT 215, 2018 [26]) suggest to calculate the shear strength of masonry panels strengthened with FRCM materials as sum of two contributions: one is the FRCM contribution provided by Equation (1). The other is the masonry contribution in case of "diagonal cracking failure", but the document does not specify which formulation has to be used (cracking in the mortar in case of regular texture or cracking in the units in case of irregular texture). Moreover, no reference to the sliding shear failure is done in the CNR document.

Since the panels investigated in the numerical analyses are made of low strength masonry blocks, the authors assume that cracks may intersect the masonry unit and the mortar joints as it is typically observed in experimental diagonal compression tests. For this reason and considering that the commentary (IBCC, 2019 36) allows to use Equation (3) for both irregular and regular masonries, it will be used for predict the shear strength of the simulated walls. In addition, Equation (3) depends on the masonry's tensile strength, f_t, which, according to the Italian code (IBC, 2018 [35]), can be directly assessed by means of diagonal compression tests.

3. Assessment of Shear Force by Means of Diagonal Compression Test

As previously discussed, diagonal compression tests are simpler to realize in comparison with shear-compressive tests, but their interpretation is more uncertain and, indeed, different approaches are available in literature (Brignola et al., 2008 [17], Alecci et al., 2012 [44], Borri et al., 2015 [45]) to calculate significant mechanical parameters of masonry, usually the tensile strength or the pure shear strength, based on the maximum applied compressive diagonal load. In this paper, an attempt to convert the maximum diagonal force in a shear force was done, since many diagonal compression tests are available in literature, while the design formulations, see Equations (1) and (3), are usually expressed in term of shear force capacity.

According to the American standard (ASTM E519 2010 [46]), the diagonal compression force applied during the test can be decomposed along the directions parallel to the wall sides (i.e., direction inclined of 45° with respect to the applied load). Such an approach assumes, indeed, a uniform shear stress distribution within the wall and, thus, the following stress state at its center (pure shear state, $\sigma = 0$, see the Mohr's circle in Figure 1b) when applied the maximum load compression load P:

$$\sigma = 0 \qquad \tau_0 = \frac{P}{A\sqrt{2}}, \tag{4}$$

in which τ_o is the shear strength corresponding to the normal stress $\sigma = 0$, and A is the area of the cross section of the wall, i.e., $A = t \cdot l$. Under these assumptions, the tensile strength of masonry, f_t, and the shear force, V_t, can be calculated as follows:

$$\sigma_I = \sigma_{II} = f_t = \tau_0, \tag{5}$$

$$\tau_0 = \frac{P}{A\sqrt{2}}, \tag{6}$$

$$V_t = \tau_0 \cdot A = \frac{P}{\sqrt{2}} \approx 0.707P, \tag{7}$$

with σ_I and σ_{II} being the tensile and compressive principal stresses, respectively.

On the other hand, RILEM guidelines (RILEM LUMB6 1994 [47]) also provide a criterion for the assessment of the stress state at the center of the panel on the basis of several experimental results obtained by Frocht (1931) [48]. Assuming the masonry wall as isotropic and homogeneous material and under linear elastic analysis, Frocht (1931) [48] found that the stress state is not uniform along the diagonal of the panel and is characterized by both shear and normal stresses as also supposed by (Brignola et al., 2008 [17], Alecci et al., 2012 [44], Borri et al., 2015 [45]). This means that the Mohr's circle relative to the center of the panel is no longer centerd in the origin (see Figure 1b). Therefore, for the tensile strength of masonry, f_t, and the pure shear strength, τ_o, i.e., the shear stress at zero normal stress, evaluated at the maximum compression force P, RILEM proposes a different interpretation, which leads to a further evaluation of the shear force V_t:

$$f_t = \sigma_I = 0.5\frac{P}{A}, \tag{8}$$

$$\tau_0 = 0.88\frac{P}{A}, \tag{9}$$

$$V_t = \tau_0 \cdot A = 0.88P. \tag{10}$$

Thus, according to RILEM interpretation, the tensile strength of masonry is lower than that provided by the ASTM standard, while the pure shear strength is higher.

Moreover, the Italian code (IBC, 2018 [35]) suggests that, in the case of diagonal compression tests, the tensile strength of masonry for diagonal cracking, f_t, can be assumed equal to the maximum diagonal applied load divided by twice the mean cross section area of the tested wall, A, i.e., it adopts Equation (5a), but it does not give any indication about the evaluation of the shear strength. Thus, two possibilities were examined in the following, starting from Equation (5a). If a pure shear stress condition, as in American standard is assumed, the shear and the tensile strength of masonry are equal; thus, the following assumptions can be done:

$$f_t = \sigma_I = 0.5\frac{P}{A}, \tag{11}$$

$$f_t = \tau_0 = 0.5\frac{P}{A}, \tag{12}$$

$$V_t = \tau_0 \cdot A = 0.5P. \tag{13}$$

Conversely, adopting the Turnšek and Čačovič criterion [41] for calculating the shear strength based on the value of tensile strength, a further different value of the shear force, V_t, can be obtained:

$$f_t = \sigma_I = 0.5\frac{P}{A}, \tag{14}$$

$$\tau_0 = \frac{f_t}{1.5} = \frac{P}{3 \cdot A}, \tag{15}$$

$$V_t = \tau_0 \cdot A = \frac{P}{3}. \quad (16)$$

Thus, basing on the result of diagonal compression tests, i.e., the maximum vertical load P, it is possible to obtain the value of the shear force, V_t, according to different approaches: Equations (7), (10), (13) and (16), which provide a wide range of variability of V_t from $0.33P$ to $0.88P$. For this reason, in the following, the reliability of these predictions will be checked by means of the comparisons with several numerical analyses concerning the simulation of diagonal compression tests on both un-strengthened and FRCM-strengthened masonry walls.

4. Summary of FE Analyses

In (Lignola et al., 2019 [15]), several simulations of the diagonal compression tests for un-strengthened and strengthened masonry walls with FRCM systems were analyzed by means of a Finite Element (FE) non-linear model implemented in the software DIANA TNO. Some masonry walls with dimensions 1 m × 1 m × 0.25 m were modeled in order to simulate the classic set-up of diagonal compression test. To this aim, two steel wedges at the two opposite corners of the wall were considered: one at the bottom representing the external full constraint and the other on the top, where the load is applied.

The study was carried out on different types of substrates, varying the mechanical properties of masonry (compressive and tensile strength, fracture energy) and of FRCM composite systems, which were made of basalt, glass, and steel fibers and were previously tested by (Bilotta et al., 2017a [7]) by means of both tensile and bond tests on masonry substrate.

4.1. Un-Strengthened Walls

Un-strengthened masonry walls were simulated in order to check the influence of the mechanical properties of masonry on the global behavior of the walls in terms of strength and ductility. Table 1 shows the mechanical parameters of the materials varied in the un-strengthened walls analyzed in DIANA (Young's modulus, E, compressive strength, f_c, tensile strength, f_t, fracture energy in tension, G_t, of the masonry substrate).

Three types of masonry, which are identified by the compressive strength, were considered, and they correspond to typical values of a natural stone, tuff (indicated with "T" in the specimen's label), very common in the South Italy, and of two types of clay bricks (B1 and B2). The values of f_c and E adopted for the different types of tuff and brick masonry reported in Table 1 are related to the values suggested in the commentary document joined to the Italian Code (IBC, 2018 [35], IBCC, 2019 [36]). Such a document provides the following ranges for the compressive strength: 1.4–2.2 MPa for irregular tuff, 2.0–3.2 MPa for regular tuff, 2.6–4.3 MPa for clay bricks. These values are indicative since they have to be divided by the confidence factor (FC), which is 1, 1.2, or 1.35, according to the knowledge level, and can be increased by coefficients greater than 1 in case of good conditions of masonry (good mortar, presence of transversal connections, presence of well-defined horizontal planes) or presence of strengthening interventions. Thus, the values of compressive strength adopted in the numerical analyses are in agreement with the possible ranges provided by (IBCC, 2019 [35]). Based on these values, the Young's modulus was calculated as $1000 \cdot f_c$.

The value of the fracture energy in tension, G_t = 0.012 N/mm, suggested in Lourenco, 1996 [27], for masonry with strength of about 5 MPa, was firstly considered for both types of masonry substrates. Keeping constant this value of G_t, the tensile strength of the masonry was varied, considering 5%, 10%, and 20% of the compressive strength. These cases are indicated in the specimen labels with the letter "W", "N", and "S", respectively.

Then, higher (10 times G_t) and lower values (0.1 times G_t) were adopted for carrying out parametrical analysis on the effect of G_t, and the following theoretical relation for G_t was also considered:

$$G_t = f_t^2 \cdot h/E \; h = \sqrt{2 \cdot A}, \quad (17)$$

where h indicates the crack bandwidth (to account for size effect) and depends on the area, A, of the finite element (10 mm × 10 mm) used in the model and on the Young's modulus, E, and tensile strength, f_t, of masonry.

Moreover, Table 1 reports the theoretical shear strength, $V_{t,th}$, given by Equation (3) for the un-strengthened walls, the values of the maximum diagonal compression force, P, given by the FE model, and the shear strength, $V_{t,FEM}$, calculated according to the Equations (7), (10), (13) and (16), based on the value of P_{FEM}. It is worth noting that, in Equation (3), $b = h/l = 1$ and $\sigma_{od} = 0$ were used.

Table 1. Theoretical and numerical results for the un-strengthened panels for different mechanical properties of masonry.

Masonry	Analysis ID	E	f_c	G_t	f_t	$V_{t,th}$	P_{FEM}	$V_{t,FEM}$ Equation (7)	$V_{t,FEM}$ Equation (10)	$V_{t,FEM}$ Equation (13)	$V_{t,FEM}$ Equation (16)
		[MPa]	[MPa]	[N/mm]	[MPa]	[kN]	[kN]	[kN]	[kN]	[kN]	[kN]
Tuff	2_T-W	1100	1.1	0.0120	0.06	15.0	80.0	56.57	70.40	40	26.67
	1_T-N				0.11	27.5	88.3	62.44	77.70	44.15	29.43
	17_T-S				0.22	55.0	88.6	62.65	77.97	44.30	29.53
Brick 1	10_B1-W	4100	4.1	0.0120	0.21	52.5	251.9	178.12	221.67	125.95	83.97
	9_B1-N				0.41	102.5	323.6	228.82	284.77	161.80	107.87
Brick 2	26_B2-N	3100	3.1	0.0120	0.31	77.5	232.7	164.54	204.78	116.35	77.57
	25_B2-S				0.62	155.0	249.5	176.42	219.56	124.75	83.17
Tuff	21_T-N-10G_t	1100	1.1	0.1200	0.11	27.5	88.5	62.58	77.88	44.25	29.50
	22_T-N-0.1G_t			0.0012			78.9	55.79	69.43	39.45	26.30
Tuff	34_T-N-Gt,th	1100	1.1	0.0016	0.11	27.5	72.8	51.48	64.06	36.40	24.27
	33_T-S-Gt,th			0.0062	0.22	55.0	88.7	62.72	78.06	44.35	29.57
Brick 2	40_B2-N-Gt,th	3100	3.1	0.0044	0.31	77.5	204.2	144.39	179.70	102.10	68.07
	39_B2-S-Gt,th			0.0175	0.62	155.0	249.8	176.64	219.82	124.90	83.27

4.2. Strengthened Walls

The analyses on in-plane strengthened walls were aimed to check the effectiveness of three types of FRCM systems (basalt and glass grids, steel cords) as the mechanical properties of the masonry substrates change (i.e., tensile and compressive strength, fracture energy in tension). In all the cases, a balanced grid was assumed embedded in a cement-based mortar with thickness of 10 mm at each side of the masonry wall. The FRCM reinforcement was, indeed, modeled by shell elements as a simplified homogeneous material considering both the contribution of the fibers and of the inorganic mortar in the constitutive behavior in tension. The real geometrical "grid" configuration of the reinforcement was not modeled (Lignola et al., 2019 [15]), and it was considered perfectly bonded to the masonry substrate, since several experimental bond tests (Bilotta et al., 2017a [7], Bilotta et al., 2017b [8]) evidenced that debonding from the substrate rarely occurs for such materials.

Figure 2 shows the experimental constitutive laws in tension of the three types of FRCM systems, i.e., a two-directional mesh made of basalt or glass fibers and a fabric made of unidirectional stainless-steel cords, used in the numerical simulations. The relations refer to the tensile stresses calculated in the whole composite cross section (grout + fibers) and are the average experimental ones obtained in tensile tests carried out on FRCM coupons (10 for each type of FRCM system) adopting the clamping-grip method by Bilotta et al., 2017a [7]. Note that the average curves are stopped at the minimum tensile strain attained within the 10 tests.

Moreover, bond tests on the same FRCM systems applied over specimens made of clay bricks evidenced that, in most cases, the maximum tensile stress attained in the bond tests, i.e., the conventional value suggested by the Italian Guidelines, was higher than the one obtained in the tensile test. This result, which seems anomalous, in reality, is related to the fact that, in the bond test, the presence of the masonry support works as a constraint to prevent "in plane" displacement of the FRCM reinforcement. Such a constraint is not present in tensile tests, which have, indeed, highlighted a significant sensitivity

of the specimens to misalignment with respect to the axis of the applied load during the test (Bilotta et al., 2017a [7], Bilotta et al., 2017b [8], Caggegi et al., 2017 [49], De Santis et al., 2017 [50], Leone et al., 2017 [51], Lignola et al., 2017 [52]).

These observations mean that the ultimate strains of the constitutive laws plotted in Figure 2 are, in many cases, safe, with respect to the conventional values related to bond tests. This is further true if the conventional strain is amplified by the factor $\alpha = 1.5$ for checks far from the anchorage, according to CNR indications (CNR DT 215 2018 [26]).

Finally, the use of the constitutive laws in tension for the FRCM materials plotted in Figure 2 means that the progressive damage in the mortar due to cracking and the eventual slippage of the fibers from the mortar are intrinsically taken into account in the numerical model, since they correspond to the real experimental behavior observed in tensile tests on coupons made of both fibers and mortar (Bilotta et al., 2017a [6]).

For the compression behavior of the FRCM systems, a constitutive law typical of a cement-based mortar was used (Lignola et al., 2019 [15]).

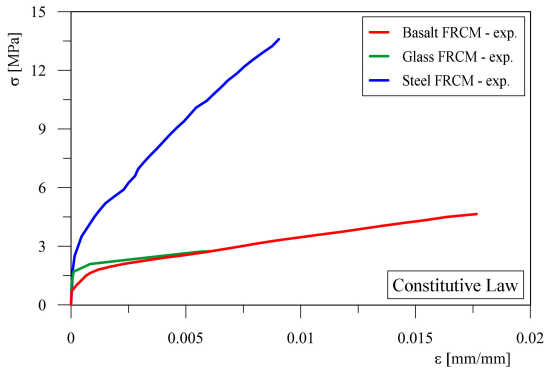

Figure 2. Fiber Reinforced Cementitious Matrix (FRCM) Constitutive Law adopted in finite element (FE) model in Lignola et al., 2019 [15].

Table 2 shows the mechanical parameters of the materials for the strengthened masonry walls analyzed in DIANA, i.e., E, f_c, f_t, and G_t, of the masonry substrate, the cross section area of the FRCM reinforcement, A_f, the ultimate strain, ε_f, evaluated according to Figure 2, and the Young's modulus, E_f, of the fibers. In all the walls, the reinforcement was applied to two sides ($n_f = 2$). Note that the letters "B", "G", and "S" in the specimen's label indicate the type of FRCM reinforcement fibers, i.e., basalt or glass fibers or steel cords, respectively. On the other hand, in Table 2, for simplicity of notation, the strengthened masonry walls were progressively renamed from 1 to 21.

It is worthy of note that all cases of strengthened walls refer to the same value of fracture energy in tension, i.e., $G_t = 0.012$ N/mm, previously introduced. Such a choice was related to the fact that, since the variation of G_t is related to the masonry behavior and it was, indeed, investigated in the un-strengthened panels, for the comparisons between the FRCM contributions provided by the FE model and ones provided by the CNR code, it was preferred to focus the attention to the variation of mechanical parameters of the FRCM reinforcement and to the tensile and compression strength of masonry, i.e., the parameters included in the code formulations.

As for the un-strengthened walls, Table 2 report the theoretical shear strength, $V_{t,th}$, for the strengthened walls, the values of the maximum diagonal compression force, P_{FEM}, given by the FE model, and the shear strength, $V_{t,FEM}$, calculated according to the Equations (7), (10), (13) and (16), based on the value of P_{FEM}.

Note that the contribution of the reinforcement to the theoretical shear capacity was calculated with Equation (1), according to Italian guideline (CNR DT 215 2018 [26]). The total shear strength, $V_{t,th}$, was thus calculated by adding the contribution of the strengthening system to the shear strength of the masonry wall given by Equation (3). Note that the assessment of the contribution of the FRCM

reinforcement requires the knowledge of the ultimate conventional strain in the fibers. To this aim, the values of $V_{t,th}$ listed in Table 2 were calculated by using the average experimental values of the ultimate strain of the fibers obtained by the tensile tests (see Figure 2). Moreover, in Equation (1), the safety factor 2 was neglected to account for mean and not design evaluations, while the coefficient α_t was assumed equal to 0.8, as suggested by (CNR DT 215 2018 [26]).

Table 2. Theoretical and numerical results for the strengthened panels for different mechanical properties of masonry and of FRCM systems.

Masonry	FRCM	Analysis ID	Case	f_t	A_f	ε_f	E_f	$V_{t,th}$	P_{FEM}	$V_{t,FEM}$ Equation (7)	$V_{t,FEM}$ Equation (10)	$V_{t,FEM}$ Equation (13)	$V_{t,FEM}$ Equation (16)
				[MPa]	[mm^2]	[–]	[GPa]	[kN]	[kN]	[kN]	[kN]	[kN]	[kN]
Tuff E = 1100 MPa f_c = 1.1MPa	B	4_T-W_B	1	0.06	39	0.018	45.3	64.93	177.4	125.44	156.11	88.70	59.13
		3_T-N_B	2	0.11				77.43	177.6	125.58	156.29	88.80	59.20
		18_T-S_B	3	0.22				104.93	180.3	127.49	158.66	90.15	60.10
	G	6_T-W_G	4	0.06	39	0.006	70.8	41.78	173.8	122.90	152.94	86.90	57.93
		5_T-N_G	5	0.11				54.28	173.9	122.97	153.03	86.95	57.97
		19_T-S_G	6	0.22				81.78	177.3	125.37	156.02	88.65	59.10
	S	8_T-W_S	7	0.06	138	0.009	146.8	308.15	243.4	172.11	214.19	121.70	81.13
		7_T-N_S	8	0.11				320.65	243.4	172.11	214.19	121.70	81.13
		20_T-S_S	9	0.22				348.15	243.3	172.04	214.10	121.65	81.10
Brick 1 E = 4100 MPa f_c = 4.1 MPa	B	12_B1-W_B	10	0.21	39	0.018	45.3	102.43	425.1	300.59	374.09	212.55	141.70
		11_B1-N_B	11	0.41				152.53	424.6	300.24	373.65	212.30	141.53
	G	14_B1-W_G	12	0.21	39	0.006	70.8	79.28	415.9	294.09	365.99	207.95	138.63
		13_B1-N_G	13	0.41				129.28	415.1	293.52	365.29	207.55	138.37
	S	16_B1-W_S	14	0.21	138	0.009	146.8	345.65	482.2	340.97	424.34	241.10	160.73
		15_B1-N_S	15	0.41				395.65	482.3	341.04	424.42	241.15	160.77
Brick 2 E = 3100 MPa f_c = 3.1 MPa	B	28_B2-N_B	16	0.31	39	0.018	45.3	127.43	338.1	239.07	297.53	169.05	112.70
		27_B2-S_B	17	0.62				204.93	338.3	239.21	297.70	169.15	112.77
	G	30_B2-N_G	18	0.31	39	0.006	70.8	104.28	335.9	237.52	295.59	167.95	111.97
		29_B2-S_G	19	0.62				181.78	336.4	237.87	296.03	168.20	112.13
	S	32_B2-N_S	20	0.31	138	0.009	146.8	370.65	402.8	284.82	354.46	201.40	134.27
		31_B2-S_S	21	0.62				448.15	402.7	284.75	354.38	201.35	134.23

B = Basalt, G = Glass, S = Steel.

5. Comparisons between Numerical Analyses and Theoretical Formulations

The reliability of the theoretical predictions can be validated through some statistical error indicators, in particular the Mean Absolute Percentage Error (MAPE), the Mean Squared Error (MSE), the slope of the best fitting line (β) passing through the origin, and the well-known Coefficient of Determination (R^2). The indicators, MAPE, MSE, and β, are calculated as follows:

$$MAPE = \frac{\sum_{i=1}^{n} \left| \frac{V_{t,FEM,i} - V_{t,th,i}}{V_{t,FEM,i}} \right|}{n}, \tag{18}$$

$$MSE = \frac{\sum_{i=1}^{n} \left(V_{t,FEM,i} - V_{t,th,i} \right)^2}{n}, \tag{19}$$

$$\beta = \frac{\sum_{i=1}^{n} \left(V_{t,FEM,i} \cdot V_{t,th,i} \right)}{\sum_{i=1}^{n} \left(V_{t,FEM,i} \right)^2}, \tag{20}$$

where n is number of available couple of data, $V_{t,FEM,i}$ is the i-th numerical shear strength calculated according to the four approaches presented in Section 3 based on the values of P_{FEM}, and $V_{t,th,i}$ is the

corresponding i-th theoretical prediction. It is worthy of note that 13 data for un-strengthened walls (Table 1) and 21 data for strengthened walls (Table 2) were considered.

5.1. Un-Strengthened Walls

For the un-strengthened walls, Figure 3 shows the comparison between $V_{t,th}$ and the shear strength given by the FE model, $V_{t,FEM}$, evaluated according to the different approaches described above and already listed in Table 2. In particular, approach 1 corresponds to Equation (7), approach 2 to Equation (10), and approach 3 to Equation (13). The best fitting lines passing through the origin are also plotted for each approach in Figure 3. Approach 4, which corresponds to Equation (16), was not considered in Figure 3, since it provides too low values in comparison with the other approaches. In Table 3, the synthetic statistical parameters MAPE, MSE, R^2, and β, previously introduced, are listed.

Figure 3 shows that, whatever approach is used, the FE results are usually higher than the theoretical predictions given by Equation (3). In particular, for approach 2, in few cases, the theoretical predictions are higher than the FE results, and, indeed the value of β is the largest among the three considered approaches (i.e., $\beta_2 = 0.86$ vs. $\beta_1 = 0.57$ and $\beta_3 = 0.46$). Conversely, the values of R^2 are the same for the three approaches since the three equations differ only for a coefficient (0.500, 0.707, 0.880); thus, the scatter of each point, $V_{t,th,i}$–$V_{t,FEM,i}$, with respect to the best fitting line of each approach, is the same.

If the results of simulations by validated FE models, i.e., numerical experiments, are considered equivalent to experimental tests (as shown in many simulations of tests on masonry with DIANA—Grande et al., 2008 [28], Lignola et al., 2012 [29], Grande et al., 2013 [30], Parisi et al., 2013 [31], Ceroni et al., 2014 [32], Garofano et al., 2016 [33]), the theoretical values should be equal to the FE predictions. This means that the "underestimation" area in the graphs of Figure 3 refers to the assumption that the theoretical predictions given by the codes without safety factors are higher than the numerical results, assumed equivalent to experimental results. In this sense, they are not unsafe from a design point of view, but by looking at the predictability of the theoretical model with average values.

However, if it is not the case, on safe side, the theoretical values (without any design safety coefficient) should be preferably lower than the FE one. This occurs in almost all cases for the three considered approaches, but approaches 1 and 2 seem to be too safe. Thus, approach 3 seems to be the most suitable approach to estimate the shear strength of the un-strengthened wall starting from the maximum compressive force attained in a diagonal compression test. Moreover, the values of MAPE and MSE for the three approaches evidence that Equation (13) provides the lowest average percentage difference between the theoretical predictions and the numerical results. Finally, looking at the slope of the best fitting lines, approach 3 seems again to be the most reliable since its fitting line is closest to the bisector because it has β = 0.86.

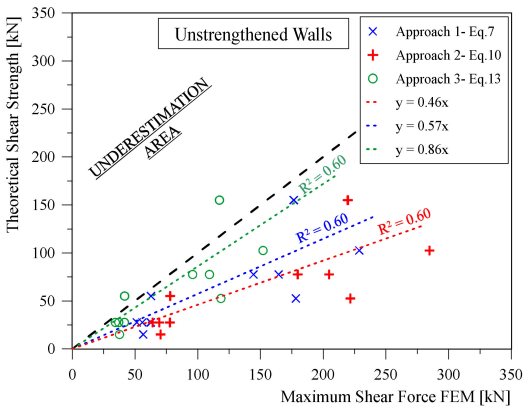

Figure 3. Theoretical shear force vs. Finite Element Model (FEM) predictions for un-strengthened walls.

Table 3. Statistical error indicators for the different approaches applied to the un-strengthened walls.

Approaches	Shear Force	Parameters			
		MAPE	MSE	R^2	β
Approach 1	$V_t = 0.71\ P$	0.43	3876	0.60	0.57
Approach 2	$V_t = 0.88\ P$	0.54	8395	0.60	0.46
Approach 3	$V_t = 0.50\ P$	0.34	953	0.60	0.86
Approach 4	$V_t = 0.33\ P$	0.37	990	0.60	1.22

5.2. Strengthened Walls

For the strengthened walls, Figure 4 shows the comparisons between the theoretical shear strength, $V_{t,th}$, given by Equations (1) and (3), and the numerical values, $V_{t,FEM}$, calculated according to Equations (7), (10) and (13) based on the maximum compression force, P_{FEM}, given by the FE analyses, i.e., the data listed in Table 2. Again, provisions given by Equation (16) are not plotted in the graphs since they are too low in comparison with the other ones.

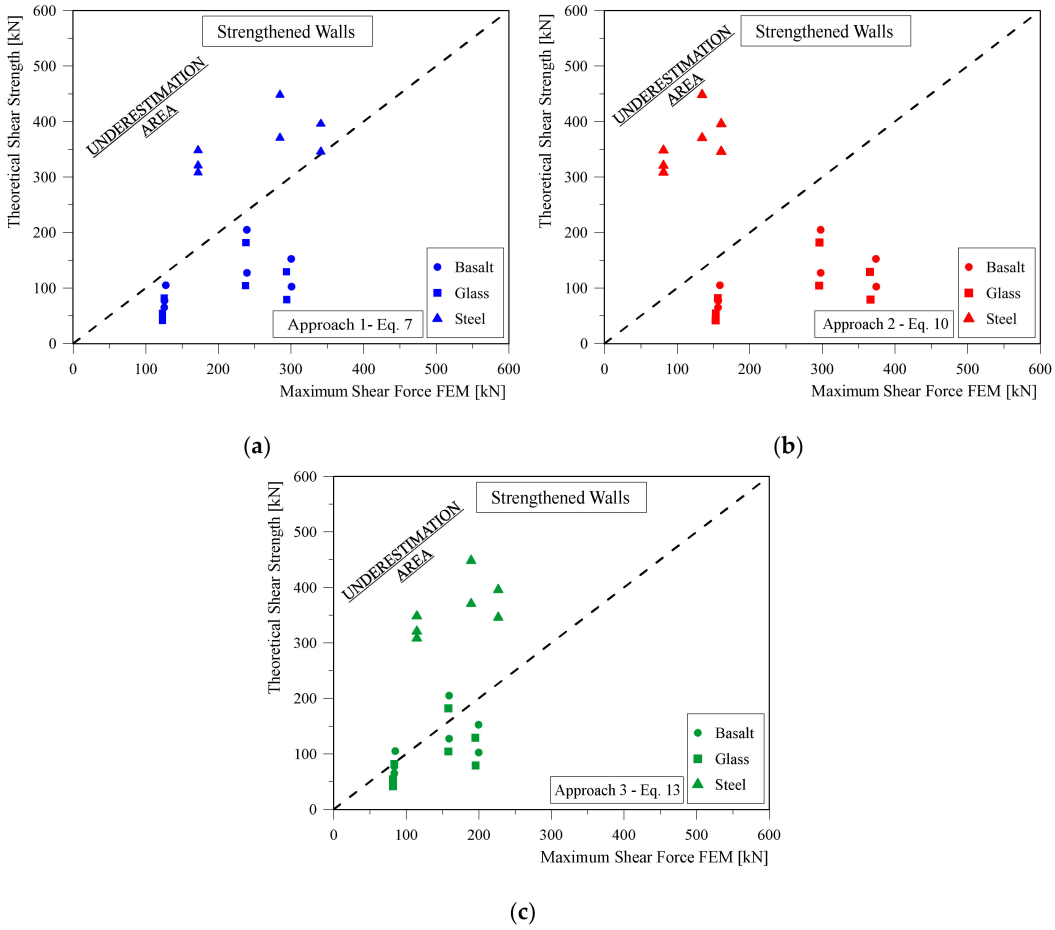

Figure 4. Theoretical shear strength vs. FEM predictions for strengthened walls: (**a**) Approach 1; (**b**) Approach 2; (**c**) Approach 3.

In general, Figure 4 shows that for the basalt and glass reinforcements the comparisons between numerical and theoretical results are always better than those related to the steel cords for whatever approach; the theoretical predictions for the steel FRCM reinforcement are, indeed, always significantly higher than the numerical ones, whatever the equation used for calculating the shear strength. Such a strong difference in terms of reliability for the three types of FRCM reinforcement makes it difficult to

evaluate which is the best fitting approach and can be related to the actual working strains of fibers, which are probably lower than the ultimate ones. Note, indeed, that the values of $V_{t,th}$ listed in Table 2 and plotted in Figure 4 are calculated by using the experimental ultimate strain of the fibers obtained in the tensile tests, but these values could not have been attained in the diagonal compression test on the strengthened walls. Therefore, the calculation of the shear capacity of the strengthened walls was again evaluated by using strain values as close to the real numerical ones as possible.

In order to correctly assess the actual strain values in the fibers when the walls fail, from the FE analysis carried out with DIANA (Lignola et al., 2019 [15]), the average fiber strain at the peak force for each simulated wall along its diagonal was identified. Figure 5 shows and justifies what emerged previously: the values of the strains attained in the fibers at the peak force in the strengthened walls are indicated on the experimental constitutive laws of each FRCM reinforcement. It is evident that, for the case of basalt fibers (Figure 5a), with the exception of a couple of points, the strains are higher than 50% of the ultimate values. Conversely, for the glass fibers (Figure 5b), the strains are sufficiently close to the ultimate values. For the case of steel cords (Figure 5c), on the other hand, it is worthy of note that the strains at the peak load are very low, on average, and, therefore, very far from the ultimate values.

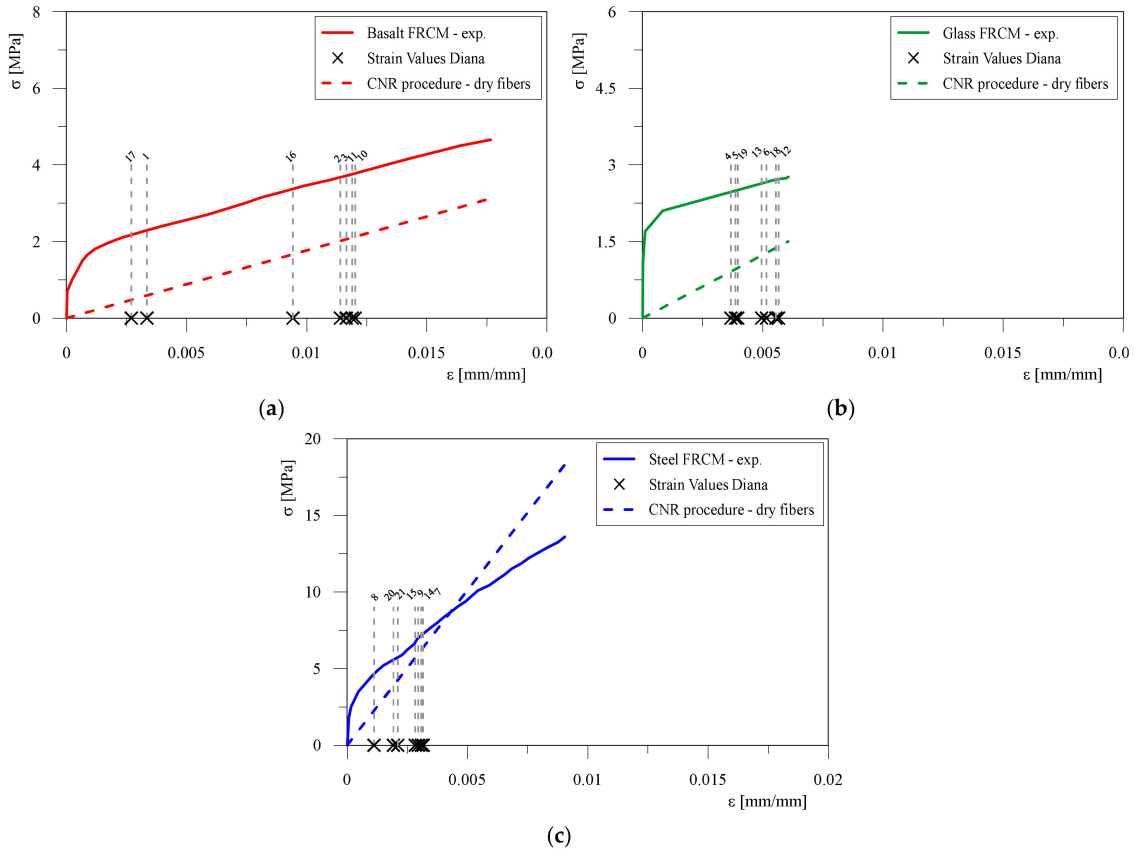

Figure 5. Evaluation of fibers strains in the strengthened walls at failure and comparisons with the constitutive laws: (**a**) basalt; (**b**) glass; (**c**) steel.

Analyzing the individual cases in detail, it clearly emerges that the range of variation of strains with reference to their ultimate value are:

1. for the case of basalt fibers, excluding two isolated cases: 53–68%;
2. for glass fibers: 61–93%;
3. for steel cords: 12–5%.

These results justify that, if the ultimate strains of the constitutive laws are used, as previously done, despite the reduction related to the use of $\alpha_t = 0.8$, the contributions to the shear strengths of the strengthened walls are clearly overestimated. Clearly, the current exploiting ratio of the fibers of FRCM reinforcement should be better assessed based on a wider database of experimental and numerical results and differentiated for FRCM typologies.

As discussed in Section 1, the conventional tensile strain suggested by the Italian guidelines (CNR DT 215 2018 [26]) should be assessed by means of bond tests and by using the Young's modulus of the dry fibers. This procedure has to be applied carefully since: (1) the maximum tensile stress in a bond test is not always lower than the maximum tensile stress attained in a tensile test (Caggegi et al., 2017 [49], De Sanctis et al., 2017 [50], Leone et al., 2017 [51], Lignola et al., 2017 [52]), as already discussed previously, and, however, if it is lower, when it is increased by 1.5 in case of checks far from anchorage, it should never become higher; (2) the values of strain calculated by dividing the tensile stress to the Young's modulus of the dry fibers are not the same that can be read in the constitutive law of the FRCM composite material, which is markedly nonlinear due to the mortar matrix tension stiffening.

Therefore, in Figure 5, the lines corresponding to the behavior of the dry fibers, i.e., depending only on their Young's modulus, are also plotted with dashed lines in order to evidence the differences in the evaluation of the strains, when the full section of the composite FRCM material, i.e., fibers + mortar, or only the section of the dry fibers is considered. Note that crossing of lines for the FRCM system made of steel cords is probably due to experimental slippage of the fibers in the mortar matrix (Bilotta et al., 2017b [8]). Since the experimental constitutive laws of the FRCM are introduced in the FE model (Figure 2), the real behavior of the composite material (fibers + mortar) is automatically taken into account in the FE model.

Based on the previous results, the shear strengths of the strengthened walls were re-evaluated using Equations (1) and (3) by updating the design values in the fibers with their effective values given by the FE analysis. Considering the graphs of Figure 5, two further cases were considered for calculating the stresses corresponding to the effective strains. Firstly, in accordance with the formulation of the Italian Guidelines, in Equation (1), the stresses were calculated by multiplying the effective strains provided by the FE analysis to the Young's modulus of the dry fibers (i.e., the stresses were read on the dashed lines of Figure 5). This procedure completely neglects the tension stiffening contribution of the mortar matrix, and the shear capacities provided in this way are indicated in Figure 6 with letter "A", i.e., "Basalt A", "Glass A", and "Steel A".

Moreover, in order to have a more realistic comparison with the FE model, which considers the effective constitutive law of the FRCM materials during the numerical simulation, the total stresses in the composite were considered by including the mortar matrix contribution. Thus, in this second case, the term $\varepsilon_{fd} \cdot E_f$ in Equation (1) was directly substituted by the tensile stress read in the constitutive laws of the FRCM systems (continuous lines in Figure 5) in correspondence of the strain attained by the in the fibers at the peak load. The shear capacities calculated according to this procedure are indicated in Figure 6 with letter "B", i.e., "Basalt B", "Glass B", and "Steel B".

For both procedures, in Equation (1), the safety factor 2 was neglected, as done previously, while the coefficient α_t was assumed equal to 1, since the effective strains in the fibers were directly assessed by means of the FEM analyses.

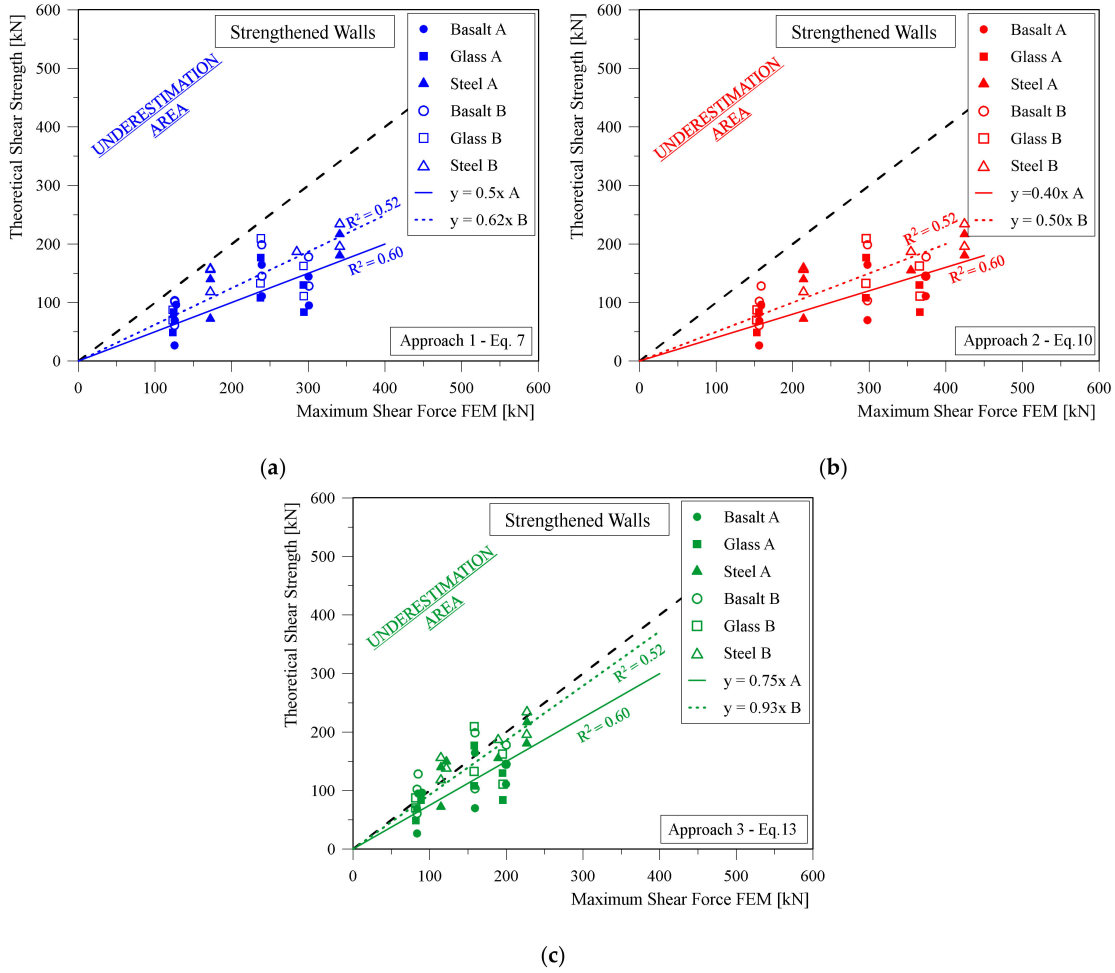

Figure 6. Comparison between theoretical shear strength and FEM predictions for strengthened walls: (**a**) Approach 1; (**b**) Approach 2; (**c**) Approach 3.

The comparisons between the theoretical and numerical predictions are shown again in Figure 6: the theoretical values are calculated by using the two procedures, A and B, for the assessment of the effective stresses in the FRCM reinforcement, while the numerical ones are the same considered in Figure 5, i.e., calculated according to the three different approaches represented by Equations (7), (10) and (13). It is worthy of note that, in all cases, the theoretical predictions of shear strength clearly reduce respect to the values plotted in Figure 4. In particular, for approach 3, a densification of the points along the bisector of the quadrant can be observed for all the types of reinforcement, emphasizing a not excessive gap between the theoretical predictions and the FEM simulations. Moreover, the cases of the walls strengthened with steel cords, which resulted strongly overestimated in Figure 4, are more reliably predicted by the theoretical formulations, thanks to the significant reduction of strains (see Figure 5c). Conversely, for approaches 1 and 2, the use of effective strains leads all theoretical predictions to become lower than the numerical ones, evidencing an excessive underestimation, especially for approach 2.

It is worthy of note that, based on Figure 5, higher values of the theoretical shear strength are obtained when procedure B was used. This result means that procedure A, i.e., the one suggested by the Italian guidelines for calculating the contribute of the FRCM reinforcement, neglecting the contribute of mortar matrix, is reasonably on the safe side.

The statistical parameters MAPE, MSE, R^2, and β were calculated again for the strengthened walls, for all the approaches and for both "A" and "B" procedures, and are listed in Tables 4 and 5.

Table 4. Statistical error indicators for the different approaches applied to the strengthened walls—procedure "A".

Approaches	Shear Force	Parameters			
		MAPE	MSE	R^2	β
Approach 1	$V_t = 0.71\ P$	0.51	15463	0.60	0.50
Approach 2	$V_t = 0.88\ P$	0.61	32894	0.60	0.40
Approach 3	$V_t = 0.50\ P$	0.30	2702	0.60	0.75
Approach 4	$V_t = 0.33\ P$	0.26	1585	0.6	1.06

Table 5. Statistical error indicators for the different approaches applied to the strengthened walls—procedure "B".

Approaches	Shear Force	Parameters			
		MAPE	MSE	R^2	β
Approach 1	$V_t = 0.71\ P$	0.35	9464	0.52	0.62
Approach 2	$V_t = 0.88\ P$	0.47	23802	0.52	0.50
Approach 3	$V_t = 0.50\ P$	0.22	1414	0.52	0.93
Approach 4	$V_t = 0.33\ P$	0.43	2273	0.52	1.32

As observed for the unreinforced walls, similar considerations can also be made for the strengthened ones: when approach 1 is used (Figure 6a), the theoretical provisions for the procedure "A" are sensibly lower than FEM, i.e., $\beta_A = 0.50$, while procedure "B" appears to be slightly better, since β is 0.62. For approach 2 (Figure 6b), similar considerations to approach 1 can be made: all points are in safe area, too far below the bisector for the procedure "A" ($\beta_A = 0.40$), while, for procedure "B", the average difference is slightly reduced ($\beta_B = 0.50$). Finally, for approach 3 (Figure 6c) and procedure "A", the theoretical predictions are lower than the numerical ones, in most cases, with low differences, i.e., $\beta_A = 0.75$, while, for procedure "B", fewer points are in safe area and, consequently, the differences are further reduced, i.e., $\beta_B = 0.93$.

On the statistical error indicators, as observed for the unreinforced walls, approach 3 is characterized by lower values of MAPE and MSE than those of approaches 1 and 2, which are also safe, but too much, as previously discussed. Furthermore, looking at the slope of the best fitting lines, approach 3 seems to be again more reliable than the others, since, despite the fact that the two fitting lines are in the safe area like as for approaches 1 and 2, they are closest to the bisector line, i.e., $\beta_A = 0.75$ and $\beta_B = 0.93$; thus, they have to be preferred over the other approaches.

Finally, all the previous considerations lead to considering approach 3 as the most suitable one both for the un-strengthened and strengthened walls.

6. Conclusions

The paper is focused on the assessment of the shear capacity of un-strengthened and in-plane FRCM-strengthened masonry walls under diagonal compression force. Previous numerical analyses carried out by means of a Finite Element (FE) Model simulating diagonal compression tests were used in the paper in order to calculate the shear strength starting from the values of the maximum diagonal compression forces. To this aim, various approaches commonly adopted for the interpretation of diagonal compression tests in terms of shear force were examined. Due to the simplicity of the set-up, several experimental and numerical results of diagonal compression tests are, indeed, available in literature.

Conversely, since codes and literature provisions for the strength capacity of masonry walls are given in terms of maximum shear force, the paper aimed to compare such theoretical values with the numerical results of diagonal compression tests and to find the most suitable approach for interpreting the results of this type of test both for the un-strengthened and the FRCM-strengthened

walls. The comparisons were based on the assumption that numerical results from validated models are equivalent to experimental ones, since several studies are already available in literature on the reliability of FE models to correctly predict the experimental outcomes.

The indication of Italian codes both for un-strengthened (IBC, 2018 [35]) and strengthened walls (CNR DT 215, 2018 [26]) were considered as reference for the comparisons.

For all the considered cases, the comparisons show that the approach assuming the shear force equal to half of the maximum diagonal compression force seems to be the most suitable. According to this approach, the theoretical values are indeed lower than the FEM predictions with a reasonable safety. This argument is based on the assumption that the results of validated FE models, i.e., numerical experiments, are considered equivalent to experimental tests; thus, the theoretical values should be equal to the FE predictions. In this sense, the theoretical values are not "safe" from a design point of view, but by looking at the predictability of the numerical results.

For the strengthened walls, a detailed analysis of the actual strain levels in the reinforcement when the strengthened walls fail was carried out, too, by means of a deep analysis of the numerical results. According to the CNR guidelines for design of interventions with FRCM materials, a conventional strain for the fibers has to be used for assessing the shear strength of the strengthened wall. To date, such a conventional strain should be assessed by means of bond tests. The numerical simulations evidenced that the effective working strains in the fibers when the strengthened wall fails are lower than the experimental maximum ones attained by the fibers in tensile tests, which for the examined FRCM systems were comparable or lower than the maximum strains attained in bond tests. Especially for the walls strengthened with steel cords, the strains in the fibers at the peak load are only 12–35% of the experimental maximum ones, while, for basalt and glass fibers, the actual exploitation of the tensile strain is higher (53–68% and 61–93%, respectively). This means that both the coefficient α_t, which takes into account the reduced exploitation of the fibers when stressed in shear, and the assessment of the conventional strain should be revised according to the type of fibers.

Moreover, the analysis of the strain level in the fibers in the strengthened walls and of the constitutive behavior in tension of the examined FRCM systems also highlighted that the mortar still gives a contribution, although the CNR guidelines neglect it and consider only the dry fibers. However, the comparisons evidenced that such an assumption does not provide a relevant underestimation of the FRCM contribution to the shear capacity of the strengthened walls.

Finally, it can be concluded that the derivation of shear force from a diagonal compression test is still debated, and this study remarked that some methods can be too safe. The reliability and general validity of the results presented in this paper can be further checked, if more studies or experimental data will be available.

Author Contributions: Conceptualization, F.C. and G.P.L.; formal analysis and investigation, G.C.; methodology, F.C. and G.P.L.; writing—original draft, G.C.; writing—review and editing, G.C., F.C. and G.P.L. All authors have read and agreed to the published version of the manuscript.

Funding: The research activities presented in the paper were carried out in the framework of the research project PRIN "Innovative Systems for the UpgRade of MasOnry structUres and Non sTructural elements (SURMOUNT)", issued by MIUR year 2017.

Conflicts of Interest: The authors declare no conflict of interest.

References

1. Cescatti, E.; Salzano, P.; Casapulla, C.; Ceroni, F.; Da Porto, F.; Prota, A. Analysis of typologies and damages in churches after Central Italy 2016–2017 seismic sequence and definition of fragility curves. *Bull. Earthq. Eng.* **2020**, *18*, 297–329. [CrossRef]
2. Council of National Research (CNR). *Guide for the Design and Construction of Externally Bonded FRP Systems for Strengthening Existing Structures—Materials, RC and PC Structures, Masonry Structures*; CNR-DT 200 R1; Council of National Research (CNR): Rome, Italy, 2013.

3. Council of National Research (CNR). *Guidelines for the Design and Construction of Externally Bonded FRP Systems for Strengthening Existing Structures—Timber Structures*; CNR-DT 201; Council of National Research (CNR): Rome, Italy, 2005.
4. Council of National Research (CNR). *Guidelines for the Design and Construction of Externally Bonded FRP Systems for Strengthening Existing Structures—Metallic Structures*; CNR-DT 202; Council of National Research (CNR): Rome, Italy, 2005.
5. D'Ambrisi, A.; Feo, L.; Focacci, F. Experimental analysis on bond between PBO-FRCM strengthening materials and concrete. *Compos. Part B Elsevier* **2013**, *44*, 524–532. [CrossRef]
6. Carozzi, F.G.; Bellini, A.; D'Antino, T.; de Felice, G.; Focacci, F.; Hojdys, L. Experimental investigation on tensile and shear bond properties of Carbon-FRCM composites applied on masonry substrates. *Compos. Part B* **2016**, *128*, 100–119. [CrossRef]
7. Bilotta, A.; Ceroni, F.; Nigro, E.; Pecce, M. Experimental tests on FRCM strengthening systems for tuff masonry elements. *Constr. Build. Mater.* **2017**, *138*, 114–133. [CrossRef]
8. Bilotta, A.; Ceroni, F.; Lignola, G.P.; Prota, A. Use of DIC technique for investigating the behavior of FRCM materials for strengthening masonry elements. *Compos. Part B* **2017**, *129*, 251–270. [CrossRef]
9. Ceroni, F.; Salzano, P. Design provisions for FRCM systems bonded to concrete and masonry elements. *Compos. Part B Eng.* **2018**, *143*, 230–242. [CrossRef]
10. Papanicolaou, C.G.; Triantafillou, T.C.; Lekka, M. Externally bonded grids as strengthening and seismic retrofitting materials of masonry panels. *Constr. Build. Mater.* **2011**, *25*, 504–514. [CrossRef]
11. Ramaglia, G.; Fabbrocino, F.; Lignola, G.P.; Prota, A. Unified Theory for Flexural Strengthening of Masonry with Composites. *Materials* **2019**, *12*, 680. [CrossRef]
12. Ramaglia, G.; Crisci, G.; Fabbrocino, F.; Lignola, G.P.; Prota, A. FRP vs. FRCM in Flexural Strengthening of Masonry. In Proceedings of the 5th Conference on Smart Monitoring, Assessment and Rehabilitation of Civil Structures, Potsdam, Germany, 27–29 August 2019.
13. Bertolesi, E.; Carozzi, F.; Milani, G.; Poggi, C. Numerical modeling of Fabric Reinforce Cementitious Matrix composites (FRCM) in tension. *Constr. Build. Mater.* **2014**, *70*, 531–548. [CrossRef]
14. Bernardi, P.; Ferretti, D.; Leurini, F.; Michelini, E. A non-linear constitutive relation for the analysis of FRCM elements. *Procedia. Struct. Integr.* **2016**, *2*, 2674–2681. [CrossRef]
15. Lignola, G.P.; Bilotta, A.; Ceroni, F. Assessment of the effect of FRCM materials on the behaviour of masonry walls by means of FE models. *Eng. Struct.* **2019**, *184*, 145–157. [CrossRef]
16. Nerilli, F.; Marfia, S.; Sacco, E. Micromechanical modeling of the constitutive response of FRCM composites. *Constr. Build. Mater.* **2020**, *236*, 117539. [CrossRef]
17. Brignola, A.; Frumento, S.; Lagomarsino, S.; Podestà, S. Identification of shear parameters of masonry s through the in-situ diagonal compression test. *Int. J. Archit. Herit.* **2018**, *3*, 52–73. [CrossRef]
18. Calderini, C.; Cattari, S.; Lagomarsino, S. Identification of Shear Mechanical Parameters of Masonry Piers from Diagonal Compression Test. In Proceedings of the 11th Canadian Masonry Symposium, Toronto, ON, Canada, 31 May–3 June 2009.
19. Magenes, G.; Calvi, G.M. In-plane seismic response of brick masonry walls. *Earthq. Eng. Struct. Dyn.* **1997**, *26*, 1091–1112. [CrossRef]
20. Parisi, F.; Iovinella, I.; Balsamo, A.; Augenti, N.; Prota, A. In-plane behaviour of tuff masonry strengthened with inorganic matrix-grid composites. *Compos. Part B. Eng.* **2013**, *45*, 1657–1666. [CrossRef]
21. Babaeidarabad, S.; De Caso, F.; Nanni, A. URM walls strengthened with fabricreinforced cementitious matrix composite subjected to diagonal compression. *J. Compos. Constr.* **2013**, *18*, 04013045. [CrossRef]
22. Ferretti, F.; Ferracuti, B.; Incerti, A.; Mazzotti, C. Diagonal Compression Tests on Masonry Panels Strengthened by FRP and FRCM. In *Structural Analysis of Historical Constructions*; Van Balen, K., Verstrynge, E., Eds.; CRC Press/Balkema: Boca Raton, FL, USA, 2016; pp. 1069–1076. [CrossRef]
23. Del Zoppo, M.; Di Ludovico, M.; Prota, A. Analysis of FRCM and CRM parameters for the inplane shear strengthening of different URM types. *Compos. Part B Eng.* **2019**, *171*, 20–33. [CrossRef]
24. Magenes, G.; Penna, A.; Galasco, A.; da Paré, M. In-Plane Cyclic Shear Tests of Undressed Double Leaf Stone Masonry Panels. In Proceedings of the 8th International Masorny Conference, Dresden, Germany, 4–7 July 2010; pp. 1–10.

25. Türkmen, Ö.S.; De Vries, B.T.; Wijte, S.N.M.; Vermeltfoort, A.T. Quasi-static cyclic in-plane testing of masonry walls strengthened with a single-sided fabric-reinforced cementitious matrix overlay and flexible anchorage. *J. Build. Pathol. Rehabil.* **2019**, *4*, 8. [CrossRef]
26. Council of National Research (CNR). *Guide for the Design and Construction of Externally Bonded Fibre Reinforced Inorganic Matrix Systems for Strenghtening Existing Structures*; CNR-DT 215; Council of National Research (CNR): Rome, Italy, 2018.
27. Lourenco, P.B. *A User/Programmer Guide for the Micro-Modelling of Masonry Structures*; University of Technology: Delft, The Netherlands, 1996.
28. Grande, E.; Milani, G.; Sacco, E. Modelling and analysis of FRP-strengthened masonry panels. *Eng. Struct.* **2008**, *30*, 1842–1860. [CrossRef]
29. Lignola, G.P.; Prota, A.; Manfredi, G. Numerical investigation on the influence of FRP retrofit layout and geometry on the in-plane behavior of masonry walls. *J. Compos. Constr.* **2012**, *16*, 712–723. [CrossRef]
30. Grande, E.; Imbimbo, M.; Sacco, E. Finite element analysis of masonry panels strengthened with FRPs. *Compos. Part B Eng.* **2013**, *45*, 1296–1309. [CrossRef]
31. Parisi, F.; Lignola, G.P.; Augenti, N.; Prota, A.; Manfredi, G. Rocking response assessment of in-plane laterally-loaded masonry walls with openings. *Eng. Struct.* **2013**, *56*, 1234–1248. [CrossRef]
32. Ceroni, F.; Garofano, A.; Pecce, M. FE Modelling of Masonry Panels Externally Bonded with FRP. In Proceedings of the 2nd International Conference on Protection of Historical Constructions (PROHITECH), Antalya, Turkey, 5–7 July 2014.
33. Garofano, A.; Ceroni, F.; Pecce, M. Modelling of the in-plane behaviour of masonry walls strengthened with polymeric grids embedded in cementitious mortar layers. *Compos. Part B Eng.* **2016**, *85*, 243–258. [CrossRef]
34. Lignola, G.P.; Di Ludovico, M.; Prota, A.; Aiello, M.A.; Cascardi, A.; Castori, G.; Corradi, M. Design Rules for In-Plane Shear Strengthening of Masonry with FRCM. In Proceedings of the 9th International Conference on Fibre-Reinforced Polymer (FRP) Composites in Civil Engineering (CICE 2018), Paris, France, 17–19 July 2018; Volume 2, pp. 114–122.
35. *Italian Building Code Aggiornamento sulle Norme Tecniche per le Costruzioni, D.M*; Italian Ministry of Infrastructures and Transportation: Rome, Italy, 2018. (In Italian)
36. *Italian Building Code Commentary, Circolare n.7 C.S.LL.PP.*; Commentary on Technical Regulations for Constructions; Italian Ministry of Infrastructures and Transportation: Rome, Italy, 2019. (In Italian)
37. De Felice, G.; Aiello, M.A.; Caggegi, C.; Ceroni, F.; De Santis, S.; Garbin, E.; Gattesco, N.; Hojdys, Ł.; Krajewski, P.; Kwiecień, A.; et al. Recommendation of RILEM Technical Committee 250-CSM: Test method for Textile Reinforced Mortar to substrate bond characterization. *Mater. Struct./Mater. Constr.* **2018**, *51*, 95. [CrossRef]
38. De Santis, S.; De Canio, G.; de Felice, G.; Meriggi, P.; Roselli, I. Out-of-plane seismic retrofitting of masonry walls with Textile Reinforced Mortar composites. *Bull. Earthq. Eng.* **2019**, *17*, 6265–6300. [CrossRef]
39. D'Ambra, C.; Lignola, G.P.; Prota, A.; Sacco, E.; Fabbrocino, F. Experimental performance of FRCM retrofit on out-of-plane behaviour of clay brick walls. *Compos. Part B Eng.* **2018**, *148*, 198–206. [CrossRef]
40. D'Ambra, C.; Lignola, G.P.; Prota, A.; Sacco, E. Comparison of different FE modeling for in-plane shear strengthening of brittle masonry with FRCM. *Key Eng. Mater.* **2019**, *817*, 65–72. [CrossRef]
41. Turnšek, V.; Čačovič, F. Some experimental results on the strength of brick masonry walls. In Proceedings of the 2nd International Brick Masonry Conference, Stoke-on-Trent, UK, 12–15 April 1970; pp. 149–156.
42. Mann, W.; Müller, H. Failure of shear-stressed masonry—An enlarged theory, tests and application to shear-walls. *Proc. Br. Ceram. Soc.* **1982**, *30*, 223–235.
43. Pubblici, I.M. *Norme Tecniche per il Calcolo, L'esecuzione ed il Collaudo Delle Strutture in Cemento Armato, Normale e Precompresso e per le Strutture Metalliche*; Italian Government: Rome, Italy, 1996. (In Italian)
44. Alecci, V.; Fagone, M.; Rotunno, T.; de Stefano, M. Shear strength of brick masonry walls assembled with different types of mortar. *Constr. Build. Mater.* **2013**, *40*, 1038–1045. [CrossRef]
45. Borri, A.; Castori, G.; Corradi, M. Determination of shear strength of masonry panels through different tests. *Int. J. Archit. Herit.* **2015**, *9*, 913–927. [CrossRef]
46. ASTM E519/E519M-1. *Standard Test Method for Diagonal Tension (Shear) in Masonry Assemblages*; ASTM International: West Conshohocken, PA, USA, 2010.
47. RILEM LUMB6. Diagonal Tensile Strength Tests of Small Wall Specimens. In *Rilem Recommendations for the Testing and Use of Constructions Materials*; RILEM: Sheffield, UK, 1994; pp. 488–489.

48. Frocht, M.M. Recent Advances in Photoelasticity. *ASME Trans.* **1931**, *55*, 135–153.
49. Caggegi, C.; Carozzi, F.G.; De Santis, S.; Fabbrocino, F.; Focacci, F.; Hojdys, Ł.; Emma Lanoye Zuccarino, L. Experimental analysis on tensile and bond properties of PBO and aramid fabric reinforced cementitious matrix for strengthening masonry structures. *Compos. Part B Eng.* **2017**, *127*, 175–195. [CrossRef]
50. De Santis, S.; Ceroni, F.; de Felice, G.; Fagone, M.; Ghiassi, B.; Kwiecień, A.; Lignola, G.P.; Morganti, M.; Santandrea, M.; Valluzzi, M.R.; et al. Round Robin Test on tensile and bond behaviour of Steel Reinforced Grout systems. *Compos. Part B Eng.* **2017**, *127*, 100–120. [CrossRef]
51. Leone, M.; Aiello, M.A.; Balsamo, A.; Carozzi, F.G.; Ceroni, F.; Corradi, M.; Gams, M.; Garbin, E.; Gattesco, N.; Krajewski, P.; et al. Glass fabric reinforced cementitious matrix: Tensile properties and bond performance on masonry substrate. *Compos. Part B Eng.* **2017**, *127*, 196–214. [CrossRef]
52. Lignola, G.P.; Caggegi, C.; Ceroni, F.; De Santis, S.; Krajewski, P.; Lourenço, P.B.; Morganti, M.; Papanicolaou, C.C.; Pellegrino, C.; Prota, A.; et al. Performance assessment of basalt FRCM for retrofit applications on masonry. *Compos. Part B Eng.* **2017**, *128*, 1–18. [CrossRef]